Detection of Ultra High Energy Neutrinos via Coherent Radio Emission

G.S. Varner*, P.W. Gorham, R.J. Kowalski, J.G. Learned, J.T. Link, S. Matsuno, P. Miocinovic, A. Romero-Wolf, M. Rosen, B. Stokes
Dept. of Physics and Astronomy, University of Hawaii, Honolulu, HI 96822, USA
J.M. Clem, P.A. Evenson, D. Seckel
Bartol Research Institute, University of Delaware, Newark DE 19716, USA
J.J. Beatty, R. Nichol, K. Palladino
Dept. of Physics, Ohio State University, Columbus OH 43210, USA
S.W. Barwick, D. Goldstein, J. Nam, A. Silvestri, F. Wu
Dept. of Physics and Astronomy, University of California, Irvine CA 92697, USA
A. Connolly, S. Hoover, D. Saltzberg
Dept. of Physics and Astronomy, University of California, Los Angeles CA 900095, USA
D. Besson
Dept. of Physics and Astronomy, University of Kansas, Lawrence KS 66045, USA
W.R. Binns, P.F. Dowkontt, M.H. Israel
Dept. of Physics, Washington University in St. Louis, St. Louis, MO 63130, USA
K.M. Liewer, C.J. Naudet
NASA Jet Propulsion Laboratory, Pasadena CA 91109, USA
B. Cai, M.A. DuVernois, E. Lusczek
School of Physics and Astronomy, University of Minnesota, Minneapolis MN 55455, USA
P. Chen, K. Reil
Kavli Institute, Stanford University and SLAC, Stanford, CA 94305, USA

Since the 1960's it has been predicted that cosmic ray protons of the highest energies must produce corresponding high energy neutrinos due to collisions with the cosmic microwave background. Both the origin and mechanism for production of these protons remain a mystery. Detection of the neutrinos, which remain unaffected by poorly-constrained galactic and inter-galactic magnetic fields, provide a useful new astronomical observation window. Moreover, Askyaryan pointed out that detection of these neutrinos via induced showers in solid, radio transparent media, would be observable at large distances due to the coherence of the radio emission. However, more than four decades later none of these predicted events have been observed. This has been due in part to the need for enormous target volumes and cost-effective ways to instrument them. Without being able to either trigger or record such transient signals in an efficient manner, detection remains elusive. We present a high-performance, cost-effective and low-power solution to this detection problem. Low-power is needed for balloon-borne detection, and this work was done in the context of the Antarctic Impulsive Transient Antenna (ANITA) high altitude balloon project. However the compact and low-cost nature of the sampling ASIC and triggering technology opens opportunities for viable, large-scale terrestrial radio neutrino detector arrays.

1. INTRODUCTION

A challenge to our detailed understanding of the evolution of the universe is the observation of the highest energy cosmic ray events. Neither their origin nor their acceleration mechanism is understood [1]. Protons of this energy cannot travel very far through the cosmic microwave background, which means they should be produced nearby. At the same time, no nearby point sources have been observed. This is a paradox.

Degradation of the flux of these ultra high energy (UHE) protons was first pointed out by Greisen, Zatsepin and Kuzmin (GZK) [2] via the process:

$$p + \gamma \rightarrow \Delta^* \rightarrow n + \pi^+ \qquad (1)$$

and where the subsequent π^+ decay chain leads to a flux of high energy neutrinos – denoted the GZK ν flux. Based upon the cosmic ray fluence observed, as plotted in Figure 1, and uncertainty in modelling the evolution of these protons through the universe, upper and lower limits on the predicted flux are indicated by the shaded band. While the number of these neutrinos is large, their small cross section requires a large instrumented volume. Existing detectors are simply too small.

A next generation of detectors, the Pierre Auger observatory [3] in Argentina and the IceCube array at the south pole [4], when completed, will start to have possible sensitivity to these events at the one per year level. The accumulation of significant statistics, and unique determination of the events as neutrino events will be difficult. Given the cost of these detectors, they are unlikely to significantly scale up in size using the same detection techniques. Unambiguous observation of these GZK neutrinos requires a new approach, and radio detection is a promising candidate.

*Presenter and corresponding author: varner@phys.hawaii.edu

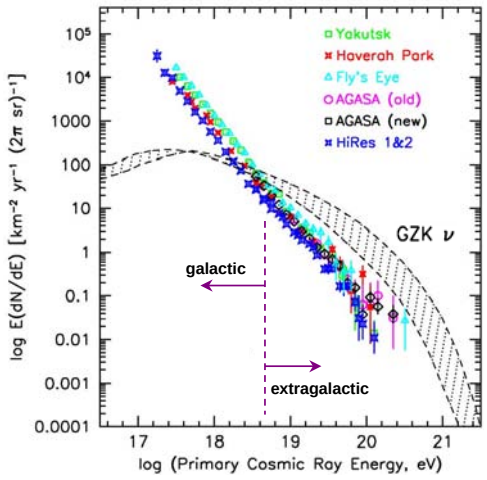

Figure 1: Measurements of the cosmic ray flux and illustration of the expected subsequent flux of GZK neutrinos.

2. COHERENT RADIO DETECTION

When neutrinos of very high energy interact in solid matter, the development of the subsequent shower progresses with electrons being Compton scattered into the shower, while positrons annihilate. This leads to a net 20-30% negative charge excess, an observation first described by Askaryan [5].

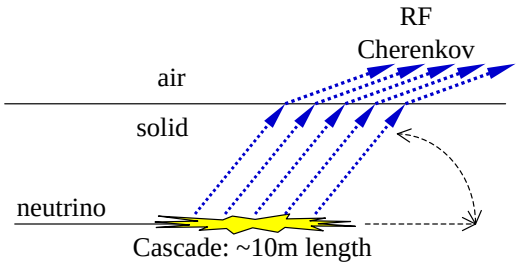

Figure 2: Radio generation in neutrino-induced showers.

He noted that such a shower, as depicted in Fig. 2, would have the following remarkable properties:

- would develop a local, relativistic net negative charge excess
- would be coherent ($P_{\rm rf} \sim E^2$) for radio frequencies
- for high energy interactions, well above thermal noise
- detectable at a distance (via antennas)
- polarized – can determine the location on Cherenkov cone with a single-point measurement

which have been experimentally verified in the last few years [6][7].

3. The ANtarctic Impulsive Transient Antenna [ANITA] Experiment

While a number of experiments have been proposed and operated based upon radio detection[8–10], their sensitivity was far away from that needed to detect the predicted GZK ν flux. This can be seen in Fig. 3, where certain models [11][12] for resolving the enigma of the highest energy cosmic rays have been constrained or ruled out.

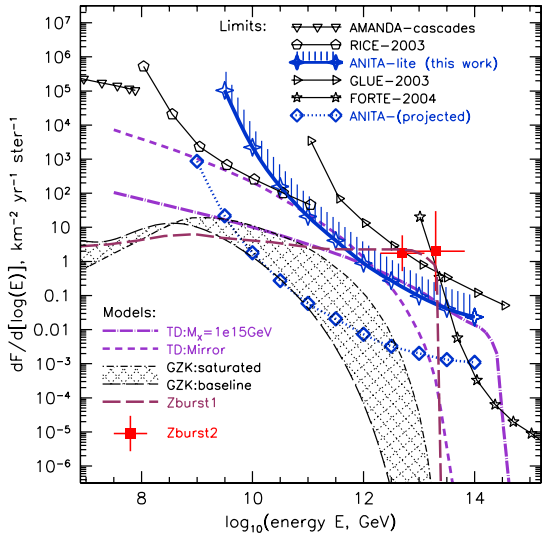

Figure 3: Present and future experimental sensitivies to the GZK flux, as well as proposed models for explaining the observed UHE proton flux.

The ANITA experiment was designed specifically to be the first to measure – or unambiguously challenge – the predicted ("guaranteed") flux of GZK neutrinos. In order to do so, the entire Antarctic ice sheet is used as a target volume, as depicted in Fig. 4.

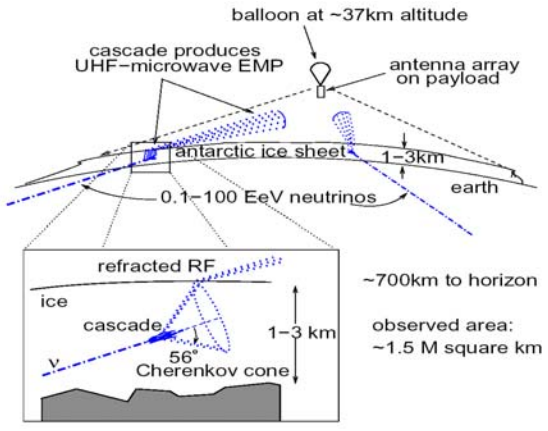

Figure 4: The ANITA concept: Antarctic ice sheet as detector and observation from a long duration balloon payload.

In order to realize this concept, a payload was designed based upon an array of quad-ridge horn antennas, as illustrated in Fig. 5.

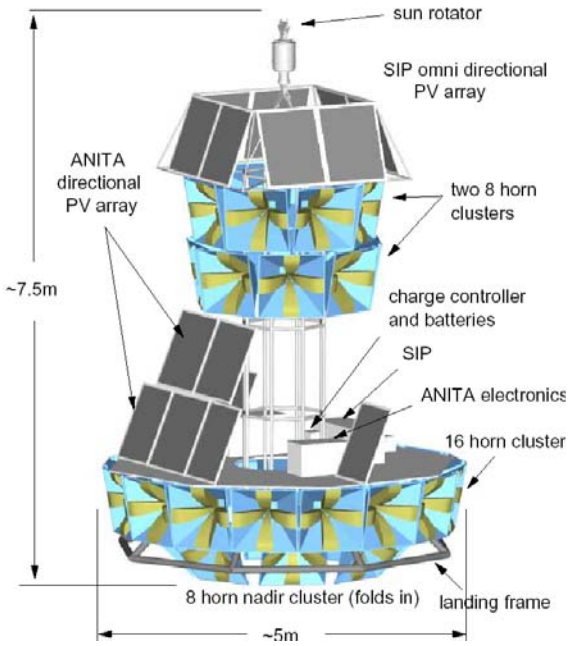

Figure 5: The ANITA payload feedhorn array.

Quad-ridge horn antennas were chosen because of their excellent frequency response over the frequency band of interest, from 0.2-1.2 GHz, and because of their tight temporal response. As the Askaryan impulses are coherent beyond the frequency of interest, the observed impulse will be band-limited, as depicted in Fig. 6.

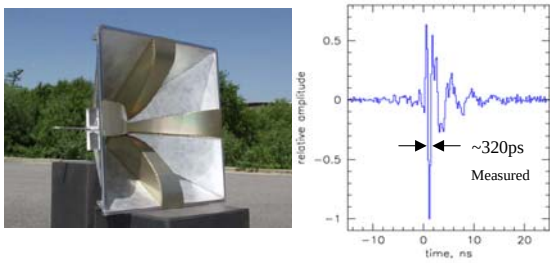

Figure 6: Quad-ridge horn antenna and its measured impulse response.

In a long-duration balloon flight primary power is solar. Just as severe is the need to eliminate the heat generated, which places practical limits of a kW or less on the entire payload.

Without being able to sample the waveforms above Nyquist frequency or trigger efficiently, there is no experiment. The demanding specifications for the low-powered electronics are summarized in Table I.

Table I ANITA Electronics Specifications.

Parameter	Quantity	Comments
# of RF channels	72	32 top, 32 bottom, 8 monitor
Sampling rate	2.6 GSa/s	greater than Nyquist
Sample resolution	$\geq$ 9 bits	3 bits noise + dynamic range
Samples in window	260	100 ns window
Buffer depth	4	allows multi-hit
Power/channel	$<$ 1W	excluding LNA, triggering
# of Trigger bands	4	equal power per band
# of Trigger channels	8	per antenna (4 bands x 2 pols.)
Trigger threshold	$\leq 2.3\sigma$	operation into thermal noise
Accidental trigger rate	$\leq$ 5 Hz	DAQ/processing limit
Raw event size	$\sim$ 35 kB	waveform samples

A divide-and-conquer strategy to address the power and performance issues raised by these specifications is shown in Fig. 7.

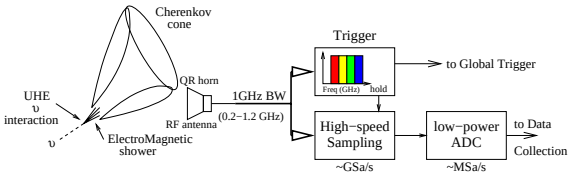

Figure 7: In order to minimize the power required, signals from the antennas are split into analog sampling and trigger paths. To provide trigger robustness, the full 1GHz bandwidth is split into 4 separate frequency bands, which serve as separate trigger inputs.

4. Triggering at Thermal Noise Levels

While an ideal flight would consist of 45 days of exposure, the total recorded livetime would still only be on the order of half a second. Therefore care must be taken to select the events of interest.

In order to provide optimal robustness in the presence of unknown but potentially incapacitating Electro-Magnetic Interference (EMI) backgrounds, a system of non-overlapping frequency bands has been adopted. Typical anthropogenic backgrounds are narrow-band, and while a strong emitter in a given band would likely raise the trigger threshold (at constant rate) such that it would be effectively disabled, the other trigger bands could continue to operate at thermal noise levels. We expect that operation at thermal noise levels means that individual trigger band channels will be firing at 1-2MHz rate. Power for and self-generated EMI from an array of 256 high-speed comparators was of great concern. To avoid large external signal swings chattering at MHz rates, it was demonstrated that the onboard FPGA could be used as the discriminator [13]. The efficiency for a

low-level impulsive signal, riding atop representative thermal noise is given in Fig. 8.

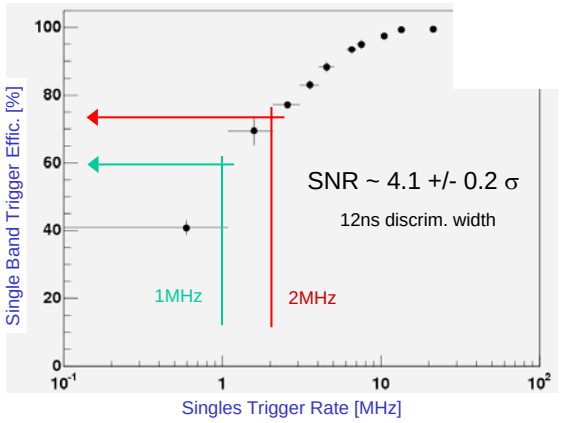

Figure 8: Measured single-band trigger efficiency versus trigger rate.

While these efficiencies may seem low, the requirement for a trigger is 3-of-8 and the net antenna trigger efficiency is given in Fig. 9.

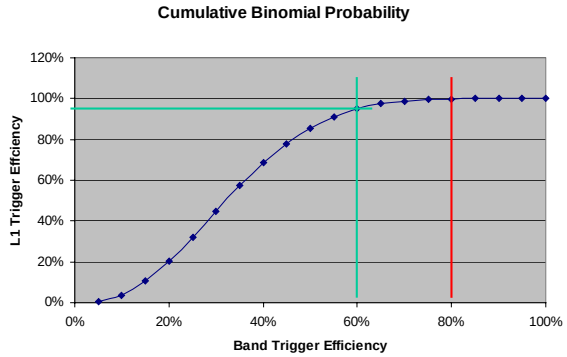

Figure 9: Cumulative binomial probability of generating an overall Antenna trigger versus the efficiency of individual band triggers.

As seen in the figure, if an efficiency of about 80% can be maintained in each band, the overall Antenna-level trigger ("Level 1" (L1)) efficiency is essentially unity. Even a degradation to 60% single band efficiency means an L1 efficiency of roughly 95%.

To get to a manageable recording rate of about 5 Hz, a multi-layer trigger system typical of a high data rate collider experiment has been adopted. Indeed, the very high effective data rates (if required to operate at those rates) would be unacceptable. Individual antenna triggers are combined as illustrated in Fig. 10. L1 (antenna) triggers are constrained to form a 2-of-5 within a ϕ cluster in each of the top and bottom clusters of antennas, and is denoted L2. A global trigger, L3, is formed by L2 coincidences between top and bottom within the same ϕ sector.

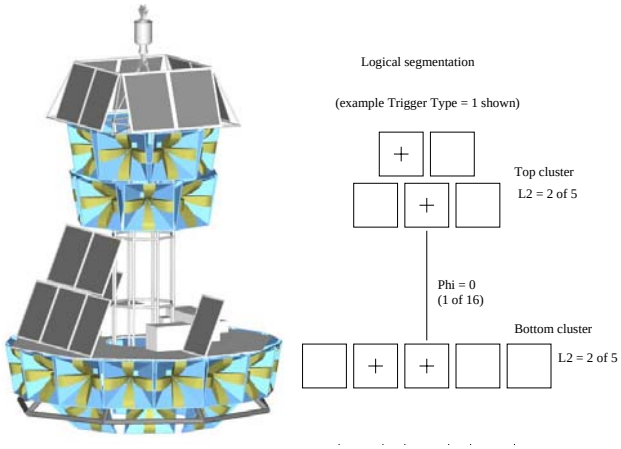

Figure 10: ANITA Multi-level trigger definition.

At the moment final integration of the ANITA payload is underway and final efficiency versus rate plots are not yet available. However, extensive simulations have been performed previously [14] which indicate that the rates should be acceptable. Sample simulation results are shown in Fig. 11, where for the coincidence window shown a rate well below 5 Hz L3 rate is maintained, as seen on the top plot. At the bottom is a conversion between sigma of noise and the units of fluctuation of the output in units of power over average power at the discriminator input.

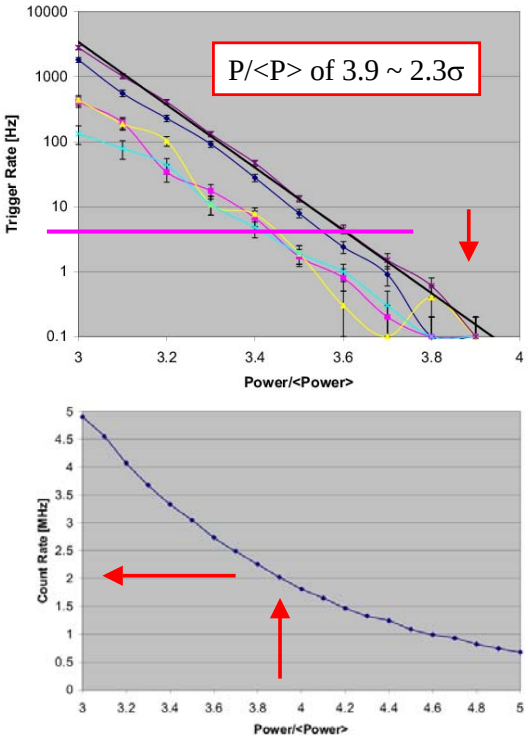

Figure 11: Monte Carlo simulation of the global L3 trigger rate for ANITA.

5. High Speed Waveform Recording

Sampling of transient impulsive events with bandwidths in excess of a GHz while maintaining low power was a major challenge. Commercial solutions are expensive, power hungry and limited dynamic range. Typical ADCs with sufficient bandwidth are only 8-bit resolution (more like 7 effective bits) and multiple Watts/channel. Therefore a custom solution was needed.

In fact, earlier Switched Capacitor Array circuits implemented in deep submicron processes [15][16] have been very successful in demonstrating that GHz sampling speeds are feasible. However, for a large number of samples there is a very basic limit given by unbuffered capacitance driven from a matched 50Ω input stripline:

$$f_{3\mathrm{dB}} = \frac{1}{2\pi Z_0 C} \qquad (2)$$

Therefore, to obtain in excess of 1.2GHz of analog bandwidth, the net capacitance must be kept to about 2pF or below. To realize this high analog bandwidth, a number of details must be considered in the design of the ASIC and package and are described in detail in Ref. [17][18]. A die photograph of this device is seen in Fig. 12.

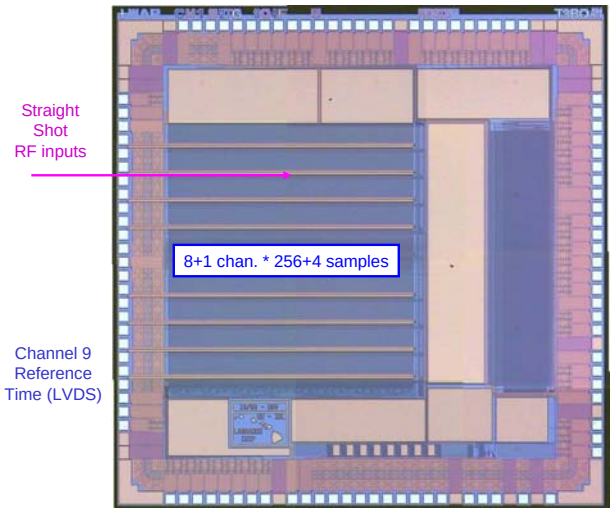

Figure 12: Die photograph of a Large Analog Bandwidth Recorder And Digitizer with Ordered Readout (LABRADOR) ASIC. This device is roughly 3 x 3 mm.

Performance of this device is demonstrated in Fig. 13, where the top figure is the recording of a raw band-limited waveform, and the bottom is the Fourier Transform, corrected for the measured spectral content of the test impulse.

The shoulder at about 200MHz is the edge of a high-pass filter upstream of the ASIC. Residual power at DC is due to an incomplete pedestal subtraction.

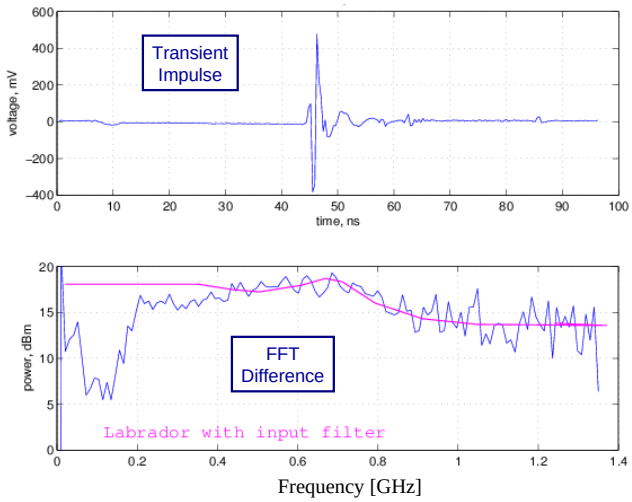

Figure 13: Waveform sampling (top) and Fast Fourier Transform (bottom) of the LAB3 ASIC response.

In summary, while the loss of input coupling above 800MHz could be improved, it is deemed to be acceptable. This is an area for improvement in future devices.

6. HIGH DENSITY PACKAGING

In order to accomodate the trigger and waveform sampling in a compact form-factor, the Sampling Unit for Radio Frequency (SURF) board was developed. A photograph of the production lot is seen in Fig. 14.

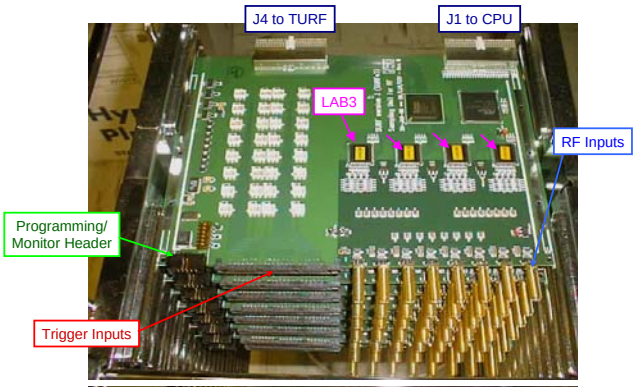

Figure 14: Photograph of the stack of production Sampling Unit for Radio-Frequency (SURF) boards.

Each SURF contains 4 LABRADOR3 sampling ASICs, to allow for multi-hit capability. Such capability is desireable to allow detection of secondary lepton showers. As the cards must reside in a conduction-cooled crate for vaccum operation, boards are shown without obligatory heat sink for clarity.

7. CONCLUSIONS AND FUTURE PLANS

After a successful prototype flight in New Mexico in September 2005, ANITA is on target for a flight from McMurdo Station, Antarctica in December 2006. Prior to this, in order to characterize the performance of the antenna array and trigger system as a detector, a beam test will be performed in the End Station A facility at SLAC in June 2006. For this experiment a solid ice target will be assembled to allow generation of Askaryan-effect showers for calibration.

For the future, the ASICs developed for waveform sampling and the techniques refined for triggering RF impulses deep into the thermal noise [19] will enable a future generation terrestrial array of embedded antennas [20]. Such a detector opens the possibility of UHE neutrino astronomy. Prototypes of such a system will be co-deployed in the IceCube array in the 2006/2007 season.

Acknowledgments

The presenter wishes to thank Stefan Ritt of PSI (Domino Ring Sampler) for useful and stimulating discussions on SCA sampling architectures. Work supported by NASA Research Opportunities in Space Science (ROSS).

References

[1] D.Seckel and T. Stanev, Phys. Rev. Lett. **95**, 141101 (2005).

[2] K. Greisen, Phys. Rev. Lett. **16**, 748 (1966); G.T. Zatsepin and V.A. Kuzmin, JETP Lett. **4**, 78 (1966).

[3] D.V. Camin *et al.* (Auger Collaboration), "Results from the Pierre Auger Observatory", EPS International Europhysics Conference on High Energy Physics (HEP-EPS 2005), Lisbon, Portugal July 2005. PoS HEP2005:027,2006

[4] C. de los Heros *et al.* (IceCube Collaboration), "Getting there: From AMANDA to IceCube", EPS International Europhysics Conference on High Energy Physics (HEP-EPS 2005), Lisbon, Portugal July 2005. PoS HEP2005:023,2006

[5] G.A. Askaryan, Sov. Phys. JETP **14**, 441 (1962); **21**, 658 (1965).

[6] D.Saltzberg *et al.*, Phys. Rev. Lett. **86**, 2802 (2001).

[7] P.W. Gorham *et al.*, Phys. Rev. D **72**, 023002 (2005).

[8] P.W. Gorham *et al.* (GLUE Collaboration), Phys. Rev. Lett. **93** 041101 (2004).

[9] N.G. Lehtinen, P.W. Gorham, A.R. Jacobson and R.A. Roussel-Dupre, Phys. Rev. D **69**, 013008 (2004).

[10] I. Kravchenko *et al.* (RICE Collaboration), Astropar. Phys. **20**, 195 (2003).

[11] S. Yoshida, H. Dai, C.C.H. Jui, and P. Sommers, Astophys. J. **479**, 547 (1997); P. Bhattacharjee, C.T. Hill and D.N. Schramm, Phys. Rev. Lett. **69**, 567 (1992).

[12] O.E. Kalashev *et al.*, Phys. Rev. D **65**, 103003 (2002); Z. Fodor, S.D. Katz and A. Ringwald, Phys. Rev. Lett. **88**, 171101 (2002); T.J. Weiler, Astopart. Phys. **11**, 303 (1999); T. Weiler, Phys. Rev. Lett. **49**, 234 (1982).

[13] G.S. Varner, "The Modern FPGA as Discriminator, TDC and ADC", submitted to JINST, arXiv:physics/0605113.

[14] ANITA Phase A proposal for the NASA Small Explorer (SMEX) program, available online: www.phys.hawaii.edu/ ∼anita/web/project/proposal/anitaprop.pdf

[15] S. Kleinfelder, "GHz Waveform Sampling and Digitization Circuit Design and Implementation", IEEE Trans. Nucl. Sci. **50**, No. 4, pp. 955-962, August 2003.

[16] S. Ritt, "The DRS chip: Cheap waveform digitizing in the GHz range.", Nucl. Instrm. Meth. **A 518**:470-471 (2004).

[17] G. Varner *et al.*, "Monolithic Multi-channel GSa/s Transient Waveform Recorder for Measuring Radio Emissions from High Energy Particle Cascades", Proc. SPIE Int. Soc. Opt. Eng. 4858-31, 2003.

[18] G. Varner, J. Cao, M. Wilcox and P. Gorham, *"Large Analog Bandwidth Recorder and Digitizer with Ordered Readout (LABRADOR) ASIC."*, manuscript in preparation for submission to Nucl. Instr. Meth. **A**, available online as **physics/0509023**.

[19] G. Varner *et al.*, "A Giga-bit Ethernet Instrument for SalSA Experiment Readout", Nucl. Instr. Meth. **A 554** (2005) 437-443.

[20] P. Gorham *et al.*, "Accelerator Measurements of the Askaryan Effect in Rock Salt: A roadmap toward teraton underground neutrino detectors.", Phys. Rev. **D 72** 023002 (2005).